International Journal of Pharmaceutics 686 (2025) 126357

Contents lists available at ScienceDirect

International Journal of Pharmaceutics

journal homepage: www.elsevier.com/locate/ijpharm

Surfactant-enriched liposomes to enhance azithromycin efficacy in *Chlamydia trachomatis* infections

Sara Lugli [a], Angela Abruzzo [a,*], Carola Parolin [a], Beatrice Vitali [a], Antonella Marangoni [b], Marielle Ezekielle Djusse [b,c], Michela Battistelli [d], Maria Laura Bolognesi [e], Teresa Cerchiara [a], Barbara Luppi [a], Federica Bigucci [a]

[a] Department of Pharmacy and Biotechnology, Alma Mater Studiorum - University of Bologna, Via San Donato 19/2, Bologna 40127, Italy
[b] Section of Microbiology, Department of Medical and Surgical Sciences (DIMEC), Alma Mater Studiorum - University of Bologna, Via Massarenti 9, Bologna 40138, Italy
[c] International PhD College, Collegio Superiore of Alma Mater Studiorum, University of Bologna, Bologna 40126, Italy
[d] Department of Biomolecular Sciences, University of Urbino Carlo Bo – Urbino, via Ca' le Suore, 2, 62029 Urbino, Italy
[e] Department of Pharmacy and Biotechnology, Alma Mater Studiorum - University of Bologna, Via Belmeloro 6, Bologna 40126, Italy

ARTICLE INFO

Keywords:
Surfactant
Liposomes
Azithromycin
Vaginal delivery
Mucopenetration
Chlamydia trachomatis

ABSTRACT

Chlamydia trachomatis is responsible for the most common bacterial sexually transmitted infection. Oral administration of azithromycin (AZT) represents the first-line treatment. However, AZT shows a low oral bioavailability, due to its poor aqueous solubility, high degradation in the stomach and incomplete absorption. To address these problems, this study aimed to develop vaginal surfactant-enriched liposomes (LP), specifically designed to improve penetration through the mucus barrier, covering the vaginal epithelium. AZT-loaded LP were prepared through the ethanol injection technique by using phosphatidylcholine in association with surfactants from the Span or Tween series. LP were characterised in terms of size, surface charge, encapsulation efficiency, stability, *in vitro* AZT release, morphology and mucopenetrating properties. Cytotoxicity on HeLa cells and antimicrobial activity against *C. trachomatis* were also assessed. LP presented different diameters and ζ-potential depending on the type of surfactant. All the formulations presented a spherical shape and were characterized by a good capacity to encapsulate AZT. Moreover, among all the formulations, Tween 80 and Span 20-containing LP provided the best AZT release profiles and were distinguished by good mucopenetrating properties. Furthermore, they remained stable over a six-month storage period. Finally, the selected LP did not show significant alteration in terms of HeLa cell viability, determining at the same time a slightly enhanced antimicrobial activity against *C. trachomatis* compared to free AZT. In conclusion, the developed formulations could be proposed as a promising platform for the local treatment of *C. trachomatis* infections, contributing to the progress in vaginal drug delivery.

1. Introduction

Chlamydia trachomatis, a Gram-negative and obligate intracellular bacterium (Wyrick, 2000), is the etiological agent of one of the most common bacterial sexually transmitted diseases. In 2020, there were an estimated 128.5 million new *Chlamydia* infections among adults (15–49 years old) globally (WHO, 2025). Infection symptoms typically may include unusual urethral and vaginal discharge, though many cases are asymptomatic. If left untreated, *Chlamydia* can cause serious health complications, including pelvic inflammatory disease and infertility in women. It also increases the risk of contracting HIV and has been associated with adverse pregnancy outcomes.

Uncomplicated *Chlamydia* infections are commonly treated with oral antibiotics such as doxycycline or azithromycin (AZT) (WHO, 2025). However, growing concerns have been raised regarding the disadvantages of oral antibiotic use. Studies have shown that these treatments can alter the homeostasis of intestinal microbiota, increasing the risk of related diseases. Moreover, the overuse of antibiotics contributes to the emergence of resistant bacterial strains, posing a significant challenge to modern medicine (Wang et al., 2023). These drawbacks highlight the

* Corresponding author at: Department of Pharmacy and Biotechnology, University of Bologna, Via San Donato 19/2, 40127 Bologna, Italy.
E-mail address: angela.abruzzo2@unibo.it (A. Abruzzo).

https://doi.org/10.1016/j.ijpharm.2025.126357
Received 1 August 2025; Received in revised form 31 October 2025; Accepted 1 November 2025
Available online 5 November 2025

need to explore alternative approaches for this vaginal infection using localized treatment. The local treatment of the disease enables the direct delivery of the drug to the site of infection, thereby enhancing therapeutic effectiveness. This approach also helps to reduce systemic absorption, thereby minimizing off-target side effects. Additionally, lower doses of antibiotics may be required compared to oral administration, reducing the risk of antibiotic resistance (Lopez-Vidal et al., 2025).

Nonetheless, vaginal drug delivery faces several challenges that must be overcome to ensure effective local drug concentration. Uniform drug distribution may be hampered by the vaginal epithelium's high degree of folding and propensity to collapse under intra-abdominal pressure. This tissue is also characterized by continuous mucus secretion that lubricates, protects, and cleanses the reproductive tract, contributing to the elimination of pathogens and foreign substances. Acting as a first line of defence, the mucus also serves as a barrier to drug delivery (Liu et al., 2021; Shapiro et al., 2022). This is especially the case for lipophilic (i.e., poorly water-soluble) drugs that interact with the lipids and glycoproteins in mucus, resulting in reduced penetration through the mucus layer and reaching the target tissue (Sigurdsson et al., 2013). Therefore, the formulation of effective delivery systems for the local delivery of poorly water-soluble drugs able to overcome the vaginal mucus barrier is of considerable scientific interest and still remains a challenge.

Among the different carriers investigated for vaginal administration of antimicrobial drugs, liposomes have garnered significant attention due to their ability to protect them from degradation, improve solubility, enhance retention at mucosal sites, and enable sustained release over extended periods (Antimisiaris et al., 2021; Vanić et al., 2025).

In the specific context of treating chlamydial infections via local vaginal drug delivery, liposome-in-hydrogel systems have been developed for the administration of resveratrol. In these systems, liposomes effectively address the compound's poor solubility and instability, thereby enhancing its therapeutic potential (Jøraholmen et al., 2020b). Additionally, AZT-loaded liposomes differing in surface charge and bilayer elasticity/rigidity (conventional, propylene glycol and deformable propylene glycol liposomes) have been evaluated to prolong drug release and localization within the vaginal tissue, while improving antibacterial activity (Vanić et al., 2019). Another notable study showed that surface-charged elastic liposomes encapsulating AZT are more effective against *C. trachomatis* infections compared to the free drug (Bogdanov et al., 2021).

On the contrary, a limited number of studies have shown the advantages of liposomes in vaginal delivery of antimicrobial drugs by exploiting better drug penetration into the mucus layer (Albash et al., 2020; Singh et al., 2017). To bridge this gap, for the first time, this study aims to design surfactant-enriched liposomes from Span and Tween series for the local treatment of vaginal chlamydial infections with AZT, a poorly soluble macrolide antibacterial agent. The poor solubility of AZT lies in its intrinsic physicochemical properties, including its high molecular weight (MW 785) and lipophilicity (log P = 3.98) (Pandey et al., 2024). The incorporation of surfactants into vesicular lipid bilayers can destabilize their structure, rendering the membranes highly flexible and elastic. This enhanced deformability enables the resulting liposomes to traverse mucus pores significantly smaller than their diameter, facilitating the delivery of encapsulated drugs across the vaginal mucosa. Owing to these properties, deformable liposomes emerge as promising candidates for the development of drug carriers capable of penetrating the mucus barrier, ensuring uniform distribution of AZT within the underlying tissue, and achieving therapeutically relevant drug concentrations. Furthermore, encapsulating AZT within liposomal carriers may enhance its solubility and enable sustained drug release, thereby contributing to improved local drug concentration and efficacy. In the context of vaginal delivery, to the best of our knowledge, up to now, only the study reported by Vanić and co-workers (Vanić et al., 2013) compared liposomes containing different surfactants. Specifically, they employed sodium deoxycholate, Tween 80 and Span 80. Within our work, for the first time, a wide range of surfactants (Span, 20, 40, 60 and 80 and Tween 40, 80 and 85) was used for the preparation of surfactant-enriched liposomes. The prepared formulations were deeply characterized to finally select those with adequate properties for vaginal application. Moreover, another point of innovation of the present study regards the *in vitro* assessment of the mucopenetration ability of AZT-loaded formulations. At the current state of the art, no scientific papers have reported the evaluation of this specific property, determining a lack of depth in the field of local treatment of vaginal diseases.

2. Materials

Phosphatidylcholine from sunflower (H90, purity ≥ 90 %) was kindly gifted by Lipoid GmbH (Ludwigshafen, Germany). Sorbitan monolaurate (Span 20, S20), sorbitan monopalmitate (Span 40, S40), sorbitan monostearate (Span 60, S60), sorbitan monoleate (Span 80, S80), polyoxyethylene sorbitan monopalmitate (Tween 40, T40), polyoxyethylene sorbitan monooleate (Tween 80, T80) and polyoxyethylene sorbitan trioleate (Tween 85, T85) were purchased from Fluka (Milan, Italy). Azithromycin dihydrate (AZT), agar, mucin type II from porcine stomach and all the solvents with analytical grade were obtained from Sigma-Aldrich (Milan, Italy). Lactic acid (80 %) was obtained from Polichimica SRL (Bologna, Italy). Lumogen red 305 (LUM) was purchased from Kremer Pigmente GmbH & Co. KG (Aichstetten, Germany).

Buffer solutions were prepared in ultra-filtered water (18.2 MΩ·cm, MilliQ apparatus by Millipore, Milford, MA, USA) as follows: 13.61 g/L KH_2PO_4 (0.1 M) for phosphate buffer at pH 4.5 used for release studies, and lactic acid 1.6 % (*v/v*) adjusted to pH 4.5 with NaOH 5 % (w/*v*) for liposome preparation. For HPLC analysis, a mixture of phosphate buffer (KH_2PO_4 0.01 M adjusted at pH 7.5 with 10 M KOH), methanol and acetonitrile (10/50/40, *v/v/v*) was used.

2.1. Methods

2.1.1. Preparation of liposomes and liposomes with surfactants

Liposomes and liposomes with surfactants were prepared by using the ethanol injection method, following the procedure previously described (Abruzzo et al., 2024), with slight modifications. Briefly, for the preparation of liposomes 200 mg of phosphatidylcholine were used, while for the preparation of liposomes with surfactants, 170 mg of phosphatidylcholine were combined with 30 mg of surfactant from Tween (T40, T80, T85) or Span (S20, S40, S60, S80) series. In both cases, the excipients were solubilised in 5 mL of ethanol for 20 min at room temperature, under magnetic stirring at 400 rpm (Arex 5 Digital, VELP® Scientifica, Monza Brianza, Italy). Due to its lipophilic nature, AZT (30 mg) was directly added to the ethanolic solution and left under stirring for 15 min more under the same conditions to ensure its complete solubilisation. To evaluate mucopenetrating properties, vesicles containing AZT and LUM (5 mg) were also prepared by including LUM in the ethanolic phase. LUM was added after AZT solubilization and left under stirring at 400 rpm for 15 min. The obtained organic solution was then injected dropwise (3 mL/min) into 10 mL of lactate buffer 1.6 % (*v/v*) at pH 4.5 and left under stirring under the same conditions for 20 min to ensure liposome formation. Then, the residual ethanol was evaporated using a rotary evaporator at 150 rpm (Laborota 4000, Heidolph Instruments, Germany) under reduced pressure (−0.8 bar) at 60 °C for 3 min.

All formulations were stored at 4–8 °C and analysed after 24 h. Vesicles were named as follows: LP for liposomes containing only phosphatidylcholine, LP-T40, LP-T80 and LP-T85 for liposomes containing surfactants from the Tween series and LP-S20, LP-S40, LP-S60 and LP-S80 for those containing Spans.

2.1.2. Determination of vesicle size, polydispersity index (PDI) and ζ-potential

Vesicle size and polydispersity index (PDI) were measured at 25 °C

by PCS (Photon Correlation Spectroscopy) using a Brookhaven 90 Plus instrument (Brookhaven Instruments Corp., Holtsville, NY, USA) with an He-Ne laser beam at a wavelength of 532 nm (scattering angle of 90°). For these measurements, vesicle suspensions were dispersed in ultra-filtered water with a dilution of 1:5000 (*v/v*). ζ-potential analysis was carried out at 25 °C using a ζ-Potential Nicomp 380 ZLS (Santa Barbara, California, USA), after a 1:1000 (*v/v*) ultrapure water dilution.

2.1.3. Determination of encapsulation efficiency

Encapsulation efficiency was assessed as previously reported (Abruzzo et al., 2024) by following the dialysis method. Briefly, 0.5 mL of vesicle suspension was placed inside a 5 cm-long dialysis tube with a molecular weight cut-off of 6–8 kDa (Spectra/Por 1 Dialysis Membrane, Spectrum Laboratories Inc., Rancho Dominguez, CA, USA) previously hydrated for 30 min in ultrapure water. The tube was then immersed in 50 mL of lactate buffer 1.6 % (*v/v*) at pH 4.5 (external phase) and kept under continuous stirring at 200 rpm for 120 min at 25 °C. After that, the external phase was withdrawn and analysed through HPLC as mentioned somewhere else (Abruzzo et al., 2024). Briefly, the chromatographic system consisted of a Shimadzu (Milan, Italy) LC-10ATVP chromatographic pump and a Shimadzu SPD-10AVP UV–vis detector set at 215 nm. Separation was performed using a Phenomenex (Torrance, CA, USA) Kinetex (150 mm × 4.6 mm I.D., 5 mm) coupled to a Phenomenex (Torrance, CA, USA) Security Guard C18 guard cartridge (4 mm x 3.0 mm I.D., 5 mm). A phosphate buffer (KH_2PO_4 0.01 M), adjusted to pH 7.5 with 10 M KOH, was prepared and filtered through 0.22 μm cellulose nitrate membrane filters (Sartorius AG, Göttingen, Germany). The final mobile phase was composed of a mixture of phosphate buffer at pH 7.5, methanol and acetonitrile (10:50:40, *v/v/v*). The flow rate was 0.8 mL/min.

The standard curve used for this purpose was obtained by solubilising AZT in methanol at concentrations ranging from 5 μg/mL to 500 μg/mL ($R^2 = 0.999$).

Encapsulation efficiency was calculated as indicated below:

$$\%EE = \frac{\text{Total amount of AZT (mg)} - \text{Amount of AZT in the external phase (mg)}}{\text{Total amount of AZT (mg)}} \bullet 100$$

2.1.4. In vitro drug release studies

The release of AZT from the different selected formulations was investigated by using a Franz-type static diffusion cells (15 mm jacketed cell with a flat ground joint and clear glass with a 12 mL receptor volume; diffusion surface area of 1.77 cm^2), equipped with a V6A Stirrer (PermeGear Inc., Hellertown, PA, USA) and a surrounding jacket, able to thermostatically control the temperature at 37 ± 1.0 °C. Vesicle suspensions (0.5 mL) were placed on mixed cellulose filters with a pore size of 0.1 μm (Millipore, Milford, MA, USA), placed between the donor and the receptor chambers. The receptor was filled with a mixture of ethanol and KH_2PO_4 0.1 M pH 4.5 (20:80, *v/v*), which mimics the vaginal pH (Giordani et al., 2019; Jøraholmen et al., 2020b). Aliquots of 0.2 mL, containing the released drug, were collected at predetermined time intervals (30, 60, 120, 180, 240, 300, 360 min) from the receptor chamber and immediately replaced with an equal volume of fresh medium. The obtained samples were properly diluted with mobile phase (1:1 *v/v*) just before HPLC analysis. A control (CTRL), obtained by dissolving AZT (3.0 mg/mL) in a mixture of water and ethanol (40:60 *v/v*), was also investigated.

Drug release over time was determined as a percentage of the Mt/M0 ratio, where Mt stands for the amount of drug released at each time and M0 is the total AZT mass loaded into vesicles. The concentration of drug released was computed from the linear regression equation obtained from dissolving AZT in a mixture of KH_2PO_4 0.1 M, pH 4.5/ethanol (80:20, *v/v*): mobile phase (1:1, *v/v*). The curve showed good linearity ($R^2 = 0.999$) and was set up with drug concentrations ranging from 0.005 mg/mL to 0.05 mg/mL.

2.1.5. Transmission electron microscopy (TEM)

The morphology and core–shell structure of vesicles in different experimental conditions were determined using transmission electron microscopy (TEM, Philips CM10, Philips Electron Optics, Eindhoven, The Netherlands) at an acceleration voltage of 80 kV and ranging from 64,000 to 130000. The TEM sample stage was prepared using a copper grid. For detailed morphological analysis, specimens were processed for TEM observation using the conventional negative staining procedure. Eighty microliters of specimen drops were deposited on formvar-carbon-coated 300 mesh grids. They were immediately fixed with 2.5 % glutaraldehyde for 1 min and then negatively stained with 2 % (*w/v*) Na-phosphotungstate for 1 min. The excess liquid of the sample was removed by filter paper and the sample dried at room temperature.

2.1.6. Mucopenetrating properties

The ability of liposomes to penetrate throughout mucin was investigated by a slightly modified method previously described (Abruzzo et al., 2021). Mucin 0.5 % (w/v) and agar 0.1 % (w/v) were dispersed in water at 100 °C and left stirring at 400 rpm until complete solubilisation. Subsequently, 3.4 mL of the obtained dispersion was poured into a 1 cm diameter syringe without a needle, properly cut with a final length of 4 cm and closed at one end with parafilm. This tube was carefully tilted at a 60° angle (Martín-Bartolomé et al., 2024; Pacheco-Quito et al., 2020). Soon after being allowed to cool down at 25 °C, 1 mL of AZT/LUM formulation was introduced at the open end of the syringe and carefully closed with parafilm. The modified syringes were kept tilted at a 60° angle at 37 °C for 4 h and immediately frozen at −20 °C overnight. After this time, the mucin-agar tubes were cut into slices of 3 mm length and stirred at 400 rpm overnight at 25 °C with 2 mL of ethanol, avoiding direct contact with light to preserve the encapsulated LUM. Afterwards, samples were treated by ultrasonication for 1 h and then centrifuged for 15 min at 11,000 rpm (Microspin 12 Centrifuge, Biosan, Latvia) to separate both the agar and the mucin from the supernatant. Absorbance of the supernatant at λ = 578 nm was then determined to evaluate the diffusion depth into the mucus of each formulation (1601 UV–Visible Spectrophotometer, Shimadzu Corporation, Australia). A control consisting of 1 mL of a 0.5 mg/mL LUM ethanolic solution was subjected to the same treatment. The collected data were compared with a calibration curve ranging from 1μg/mL to 10 μg/mL obtained under the same conditions ($R^2 = 0.995$).

2.1.7. Formulation stability

The physical stability of the selected formulations was evaluated over a storage period of 6 months at + 4–8 °C. After 1, 3 and 6 months, the samples were diluted as mentioned in Section 2.1.2 and characterised for their size and PDI using PCS, and for ζ-potential using a ζ-sizer. Furthermore, to evaluate the ability of the formulations to maintain the drug trapped within the vesicle structure over time, the EE % was assessed after 6 months of preparation as described in section 2.1.3.

Additionally, to obtain a more detailed overview of the stability of the selected formulations, assessments of sizes and ζ-potential were also

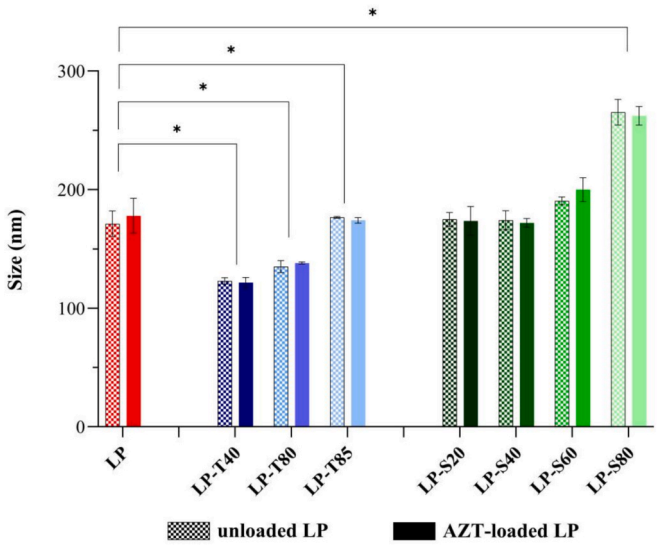

Fig. 1. Size of unloaded and loaded formulations. Data are expressed as means ± SD, n = 3. Significance indicated by * = $p < 0.05$.

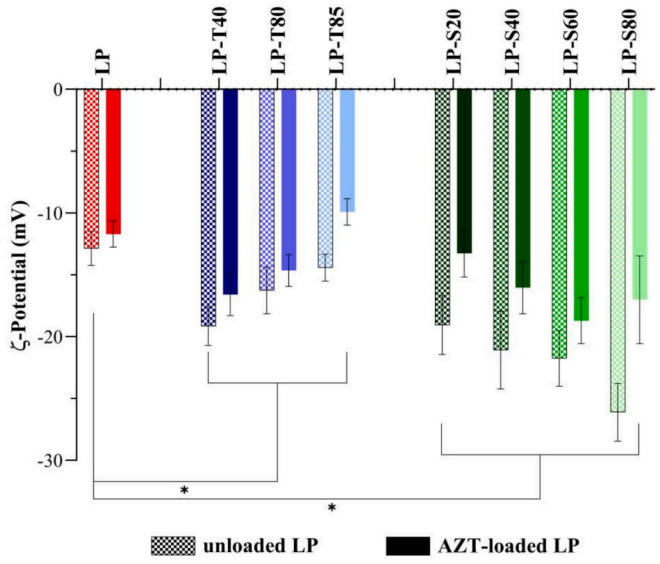

Fig. 2. ζ-potential of unloaded and loaded formulations. Data are expressed as means ± SD, n = 3. Significance indicated by * = $p < 0.05$.

carried out at the vaginal physiological pH conditions (Briuglia et al., 2015). In particular, 1 mL of each formulation, LP, LP-T80 and LP-S20 was mixed with 4 mL of KH_2PO_4 0.1 M pH 4.5, mimicking the vaginal pH (Giordani et al., 2019; Jøraholmen et al., 2020b). Subsequently, the samples were placed at 37 °C and analyzed in terms of size and ζ-potential at pre-fixed time intervals (0, 180, and 360 min).

2.1.8. Cell line and Chlamydia trachomatis (CT) strains

An immortalized epithelial cell line derived from a human cervix adenocarcinoma, HeLa (ATCC® CCL-2) was utilized in this study. HeLa cells were selected as they represent the reference *in-vitro* model for *C. trachomatis* infection studies and are widely used to investigate host–pathogen interactions (Filardo et al., 2022; Kim et al., 2025; Walker and Derré, 2024). The cells were routinely maintained in Dulbecco's Modified Eagle Medium (DMEM; EuroClone, Pero, Italy), supplemented with 10 % fetal bovine serum (FBS) and 1 % L-glutamine, in the absence of antibiotics, at 5 % CO_2 at 37 °C.

Two different CT strains were used for the experiments: GO/86 (serovar D) and LGV/17 (serovar L2). Both strains were isolated from clinical samples submitted to the Microbiology Unit of Sant'Orsola-Malpighi Hospital of Bologna (Italy), for routine diagnostic procedures and belong to the laboratory collection (Foschi et al., 2019; Nardini et al., 2016). In particular, GO/86 was isolated from a urethral swab of a patient with non-gonococcal urethritis and a serovar L from a rectal swab of a patient suffering from LGV proctitis. The purification of elementary bodies (EBs) and the evaluation of the infectivity titer expressed as inclusion forming units (IFUs)/mL, have been described elsewhere (Li et al., 2005).

2.1.9. Cytotoxicity assay

Before assessing anti-chlamydial activity, free AZT (drug solution in ethanol/water 60:40 *v/v*), AZT-loaded liposomes (LP, LP-T80, LP-S20), unloaded liposomes (unloaded LP, unloaded LP-T80, unloaded LP-S20), and lactate buffer (same medium used for liposome preparation) were tested for cytotoxicity on HeLa cells by MTT assay (De Gregorio et al., 2020). Briefly, HeLa cells were seeded in 96-well plates at 2×10^5 cell/cm^2 and allowed to grow for 24 h. Then, cells were treated with different concentrations of free AZT, liposomes and lactate buffer; dilutions corresponding to 0.94–30 mg/mL of AZT were tested. Untreated cells were used as control. After 48 h of treatment, medium was discarded and replaced with 110 µL of 3-(4,5-Dimethyl-2-thiazolyl)-2,5-diphenyl-2H-tetrazolium bromide (MTT) solution (0.5 mg/mL) in DMEM, plates were incubated for 4 h at 37 °C with 5 % CO_2. The formed formazan crystals were dissolved in isopropanol and quantified by optical density (OD) at 570 nm by EnSpire Multimode Plate Reader (PerkinElmer Inc., Waltham, MA, USA. Residual cell viability was calculated in percent as follows:

$$\text{cell viability (\%)} = \frac{\text{OD}sample}{\text{OD}control} \bullet 100$$

2.1.10. Evaluation of anti-chlamydial activity

The antimicrobial properties of the following samples were investigated: free AZT (drug solution in ethanol/water 60:40 *v/v*), AZT-loaded liposomes (LP, LP-T80, LP-S20), unloaded liposomes (unloaded LP, unloaded LP-T80, unloaded LP-S20) and the medium in which the liposomes were prepared. Different batch preparations of the selected liposome formulations were tested.

For each experiment, the HeLa cells were seeded in individual tubes containing sterile coverslip slides (Thermo Fisher Scientific, Waltham, MA, USA) to confluent monolayers of total cell number of approximately 5×10^5. They were further inoculated with a total of 5×10^3 IFUs of CT strain. Specifically, an aliquot of EBs of CT stored at −80 °C was gradually thawed in ice, vortexed and diluted in DMEM medium to a concentration of 5×10^4 IFUs/mL, 100 µL (corresponding to 5×10^3 IFUs) was added to each individual tube containing 900 µL of antibiotic-free medium, then centrifuged at 640 × g for 1 h. At the end of the centrifugation, culture medium was replaced with medium containing scalar concentrations of the different samples and incubated at 37 °C with 5 % CO_2 for 48 h. The concentrations tested for each compound ranged from 0.001875 to 0.48µg/mL with a 2-fold dilution series. After incubation, cells were washed with PBS, fixed with methanol and stained with a FITC-conjugated anti-chlamydial polyclonal antibody (Chemicon®, Merck KGaA, Darmstadt, Germany). Evans blue was used as a counterstain (0.01 % w/v). Infected cells untreated with the tested compounds were used as controls.

To estimate the rate of CT infection, the slides were observed under an epi-fluorescence microscope (Eclipse E600, Nikon, Tokyo, Japan). The number of IFUs was counted in 30 randomly chosen 200 × microscopic fields. The minimal inhibitory concentration (MIC) was defined as the lowest concentration able to reduce the number of chlamydial inclusions > 90 %, compared to the control (Foschi et al., 2018).

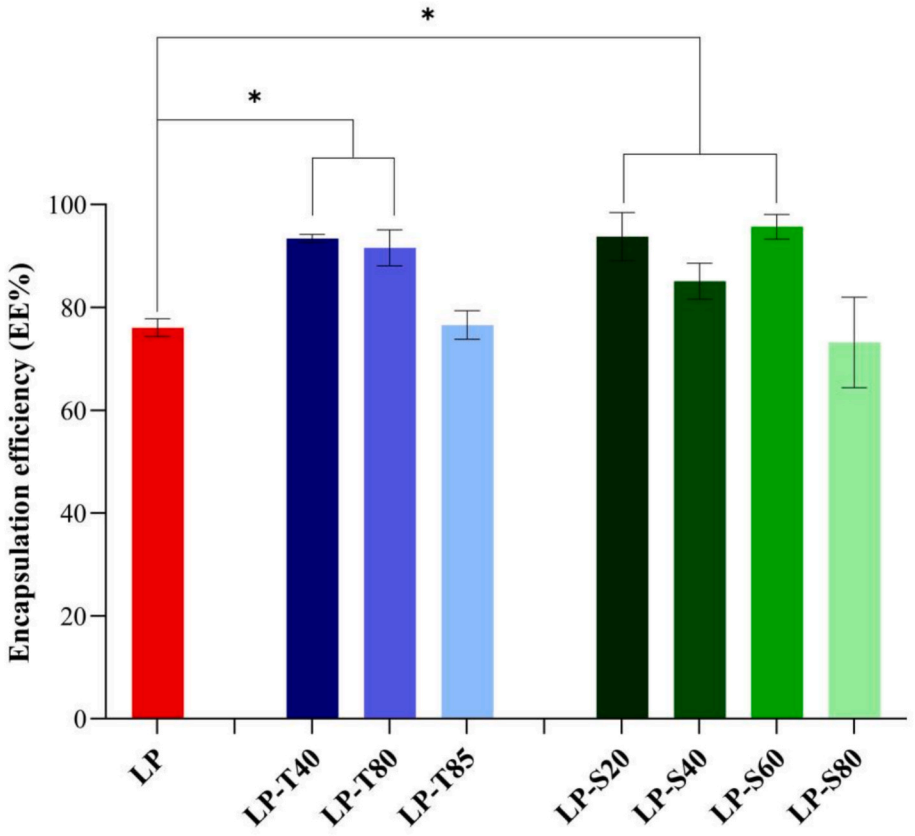

Fig. 3. Encapsulation efficiency of loaded formulations. Data are expressed as means ± SD, n = 3. Significance indicated by * = $p < 0.05$.

2.1.11. Statistical analysis

The tests here reported were performed in triplicate, except for cytotoxicity studies which were performed in four replicas. All the data are expressed as mean ± SD. *T-test* and Two-way ANOVA, followed by Tukey correction for multiple comparisons, were used to determine the studies' statistical significance. All statistical analyses were performed using GraphPad Prims version 9.5.0 for Windows (GraphPad Software, San Diego, CA, USA, https://www.GraphPad.com), and the criterion for statistical significance was $p < 0.05$.

3. Results and discussion

3.1. Determination of vesicle size, polydispersity index (PDI) and ζ-potential

The evaluation of the physicochemical properties of vesicles is of great importance since these strictly affect the drug release property, the ability to counteract microorganisms and consequently the therapeutic efficacy, as well as the final stability of the formulations.

Moreover, physicochemical properties, such as particle size and ζ-potential, play an essential role in the diffusion behaviour of vesicles through the mucus. Usually, in the field of vaginal delivery, vesicles with sizes smaller than 500 nm are found to penetrate mucus easily, improving the delivery of the antimicrobial drug to the vaginal epithelium (Rossi et al., 2019).

Within this study, liposomes and liposomes with surfactants were prepared with the final aim of developing mucopenetrating vesicles. Vesicles were developed by employing the ethanol injection technique, which ensured obtaining small and unilamellar vesicles, in agreement with our previous findings (Abruzzo et al., 2024). Additionally, this procedure is extremely rapid and easy to reproduce, with a great potential for scalability, which can facilitate large-scale manufacturing. Considering that vaginal microbiota physiologically produces lactic acid, contributing to determine a local pH around 4.5, a lactic acid solution with the same pH value was employed for the preparation of vesicle suspensions (Jøraholmen et al., 2020a; Refai et al., 2017; Tidbury et al., 2025; Yasin et al., 2002). As regards the composition of the formulations, the adequate amount of surfactant to be included in the liposomes was selected with the final aim to obtain mucopenetrating vesicles with suitable properties in terms of encapsulation efficiency, as described in the following section. As can be seen from Fig. 1, all the developed formulations (unloaded and loaded) showed sizes around 200 nm. Obtaining vesicles with mean diameters below the average mucus mesh pores, which is around 350 nm (Boegh and Nielsen, 2015), could increase the probability of vesicles diffusing deeper into the mucus layer. Additionally, thanks to the addition of surfactants, it is possible to enhance their flexibility, facilitating their transport through this barrier (Kanojiya et al., 2025). Regarding the unloaded samples, smaller vesicles were produced after the addition of T40 (123.1 ± 2.7 nm) and T80 (135.1 ± 5.1 nm), in comparison to LP (171.3 ± 10.8 nm; $p < 0.05$). Tweens are polysorbates and are classified as non-ionic surfactants with noteworthy hydrophilic characteristics. In particular, the hydrophilic-lipophilic balance (HLB) values of T40 and T80 are 15.6 and 15, respectively. The hydrophilic moiety can successfully cover the surface of the vesicles, reducing the interfacial tension that occurs in the external aqueous environment in agreement with studies conducted by previous researchers (Abdelbary and El-gendy, 2008; Bnyan et al., 2019; Duangjit et al., 2014; Liu et al., 2013), leading to small vesicles ((Khan et al., 2021; Squittieri et al., 2023). Following this behaviour, LP-T40 vesicles were smaller than LP-T80 ($p < 0.05$). Furthermore, surfactant structure impacts the final vesicle size. It was reported that surfactants with shorter alkyl chains provided smaller diameters, due to their reduced hindrance (Abdelbary and El-gendy, 2008). In addition, surfactants with unsaturated fatty acid chains may not properly fold, leading to less tight packaging and thus increasing the size (Khan et al., 2021). Results obtained in our study agreed with these observations. In

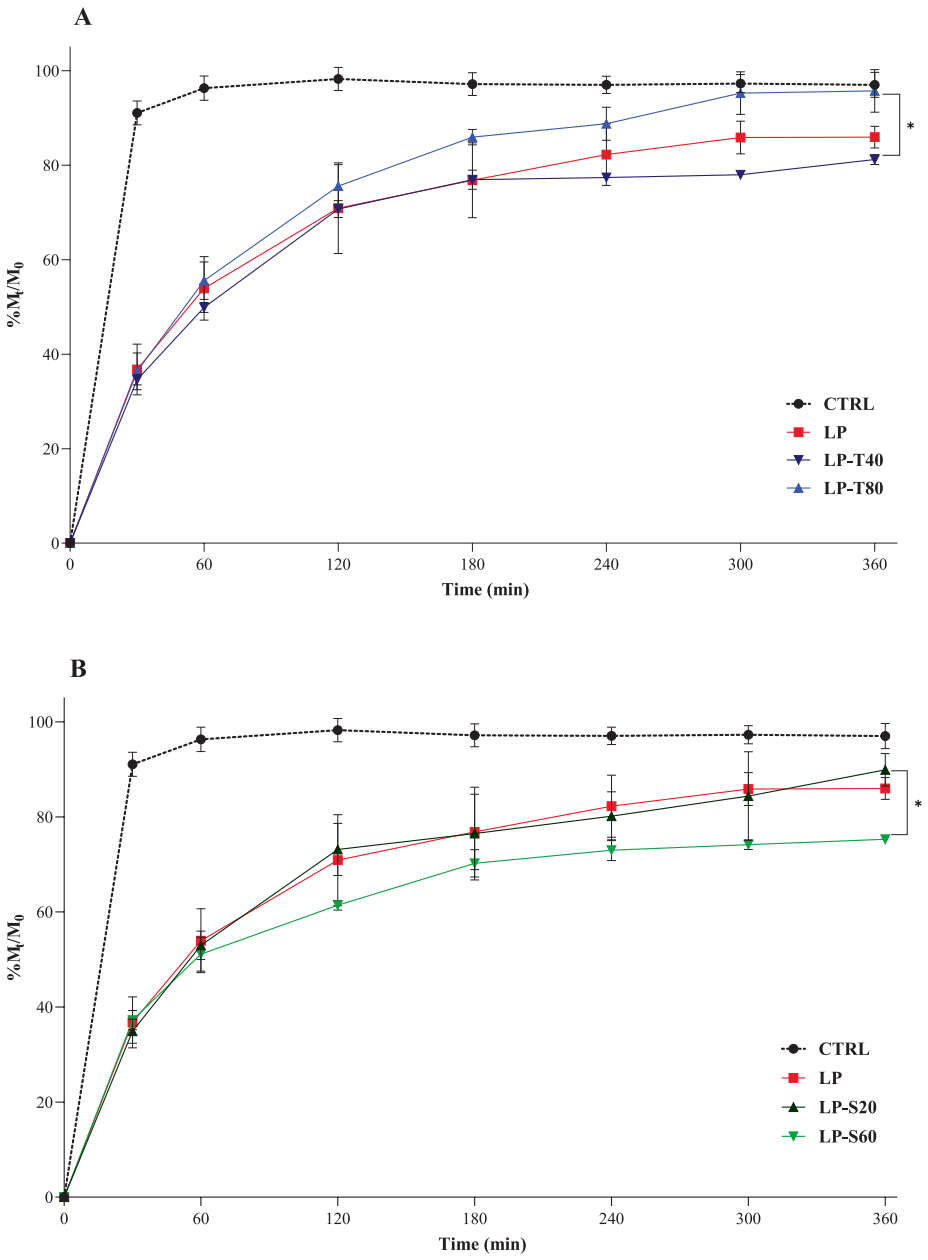

Fig. 4. Drug release profile, plotted as % Mt/M0 as a function of time, from CTRL, LP and LP with surfactant from the Tween (A) and Span (B) series. Data are expressed as means ± SD, n = 3. Significance indicated by * = $p < 0.05$.

fact, among all Tween-based formulations, the presence of Tween 40 (composed of a saturated fatty acid, e.g. palmitic acid, C_{16}) enabled the smallest vesicle sizes, while Tween 85 (composed of three unsaturated fatty acids; oleic acid, C_{18}) determined the highest increase in size. On the contrary, the Span containing vesicles showed similar mean diameters with respect to LP ($p > 0.05$), except for LP-S80 (265.4 ± 10.8 nm). This could be related to the behaviour of Spans, presenting lipophilic characteristics, which allow them to be located within the phospholipid bilayer (Khan et al., 2021) without influencing vesicle size. Spans are sorbitan esters with fatty acids classified as non-ionic and hydrophobic surfactants. Specifically, Span 20 presents an HLB value of 8.6, Span 40 of 6.7, Span 60 of 4.7 and Span 80 of 4.3. Moreover, Span 20, 40 and 60 are characterised by the presence of laurate (C_{12}), palmitate (C_{16}) and stearate (C_{18}), respectively, while Span 80, thanks to the presence of oleic acid, is the only one in this series distinguished by an unsaturated bond. As mentioned above, the size of vesicles increased with the increase of the chain length and the presence of unsaturated bonds. As can be seen from Fig. 1, LP-S20 (174.9 ± 5.6 nm) were characterised by the smallest diameter, while LP-S80 presented the biggest one. Loaded vesicles presented the same trend observed for the unloaded formulations, and no significant difference was observed in size measurements ($p > 0.05$), in agreement with previous observations (Onyesom et al., 2013). Overall, considering the final aim of this study, that of ensuring suitably small dimensions to allow the passage of vesicles through the mucus meshwork, from a merely dimensional point of view, all of them could be suitable since they ranged below 350 nm (Zheng et al., 2025).

PDI values for all the developed formulations (both unloaded and loaded) remained lower than 0.3 (data not shown), suggesting the obtainment of monodispersed vesicles.

ζ-potential is a crucial parameter since it affects both the formulation's stability and its passage through the mucus. In the first case, markedly negative or positive ζ-potential values can help to increase repulsion between vesicles, preventing aggregation phenomena and

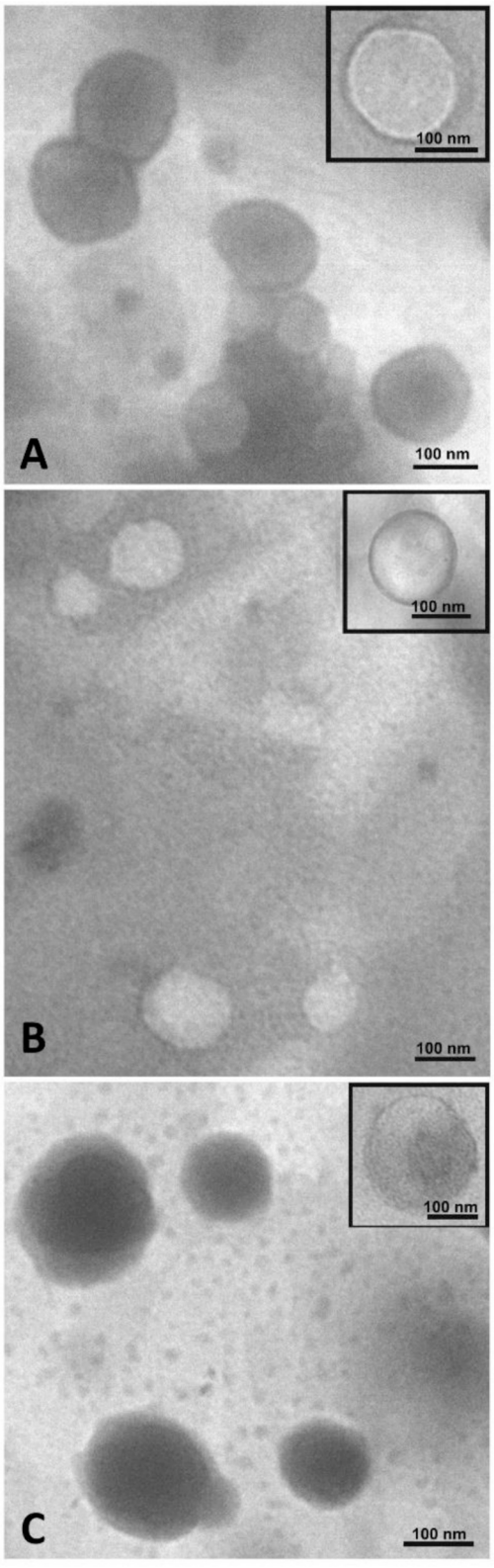

Fig. 5. Transmission electron microscope images of LP (A), LP-T80 (B), and LP-S20 (C).

increasing their stability. Secondly, considering the prevalence of negative charges of the main components of the mucus layer, positively charged nanoparticles tend to interact with them, getting trapped within the mucus, while slightly negative or near-neutral nanocarriers could diffuse and penetrate among the mesh more easily (Abruzzo et al., 2021; Rossi et al., 2019; Zheng et al., 2025). Fig. 2 reports the ζ-potential values of both unloaded and loaded formulations. As can be seen, all the unloaded formulations presented negative charges on their surfaces, with ζ-potential values ranging from −12.14 ± 1.98 mV for LP to −26.10 ± 2.33 mV for LP-S80. The obtained data can be attributed to the vesicle composition. Specifically, phosphatidylcholine is a zwitterionic species, with an isoelectric point around 6–7. Therefore, at the pH of preparation, the substance is characterised by a weak negative charge, close to neutrality, as evidenced by the LP value obtained. Upon the addition of surfactants, more negative ζ-potential values were assessed. Particularly, for the Tween series, the values changed being LP-T40 (−19.2 ± 1.6 mV) more negative than LP-T80 (−16.3 ± 1.9 mV) and LP-T85 (−14.4 ± 1.1 mV; $p < 0.05$). In general, as previously reported (Barbalho et al., 2024) Tweens shared the hydrophilic polyethylene groups, bringing the negative charges of oxygen atoms on the vesicle surface. Specifically, decreasing the HLB value, the superficial charge increases. This effect is added to the ability of the polyoxyethylene head group to create a steric hindrance that can prevent the adsorption of ions from the surrounding medium (Tasi et al., 2003).

Regarding the Spans series, the more negative ζ-potential observed with respect to LP can be attributed to the possible self-deprotonation of Spans and the formation of ionic impurities, in agreement with previous findings (Kopermsub et al., 2011; Squittieri et al., 2023). Moreover, LP-S80 (−26.1 ± 2.3 mV) gave the most negative ζ-potential value, followed by LP-S60 (−21.8 ± 2.3 mV), LP-S40 (−21.1 ± 3.2 mV) and LP-S20 (−19.1 ± 2.4 mV). This behaviour can probably be attributed to the length of the alkyl chain of the surfactant. As a matter of fact, S80 and S60, presenting the longest chains, can be included more closely within the bilayer, consequently determining the exposure of the ionic groups of phosphatidylcholines, on which the absorption of hydroxyl ions can occur (Bnyan et al., 2018; Crisóstomo et al., 2022).

After the inclusion of AZT, all vesicle surface charges moved to less negative values, mainly due to the presence of the positively charges of the drug (pKa = 8.5) located on the vesicle surface. Within the Tween or Span series, loaded vesicles showed a similar trend with respect to the unloaded ones.

Overall, the negative electrostatic charges of these lipid vesicles could enable the passage through the negative mucus. Furthermore, even if they are not highly negative, the presence of Tweens and Spans, thanks to their steric hindrance, could contribute to avoiding aggregation, improving their stability over time (Hofland et al., 1993).

3.2. Encapsulation efficiency

Achieving a good encapsulation efficiency (EE) is considered one of the main goals for the development of a successful drug delivery formulation. Fig. 3 shows the EE% of the developed vesicles. As can be seen, EE% of LP was equal to 76.1 ± 1.7 %. In our previous study (Abruzzo et al., 2024), liposomes containing AZT and phosphatidylcholine (7 mg/mL) had been developed by using two different techniques, the thin film hydration and the ethanol injection. Liposomes obtained with the ethanol injection had shown a low EE% (lower than 55 %). Indeed, to improve the EE, in this study we used a higher amount of phosphatidylcholine (20 mg/mL) with respect to the previous work. As reported in literature, by increasing the amount of lipids, it is possible to enhance the EE (Ullmann et al., 2021). Results obtained in our present study actually confirmed these findings, since by using a final phosphatidylcholine concentration equal to 20 mg/mL, we managed to obtain encapsulation efficiency higher than 75 %.

To achieve a further improvement of the EE, the adequate weight ratio between the phosphatidylcholine and the surfactant was properly selected, on the basis of previous studies. Particularly, the EE generally increases with increasing surfactant concentration. However, when surfactant content is higher than 20 % (with respect to the total excipient composition), a decrease in EE was observed (Gupta, 2012). Taking into account all these findings, we selected the weight ratio between the

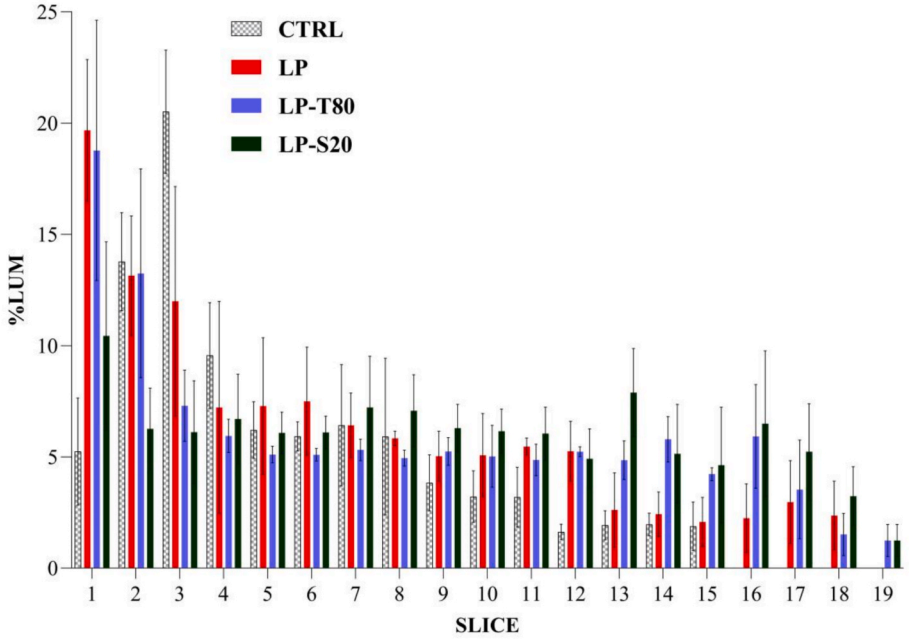

Fig. 6. % Lumogen (LUM) in each slice from the control and the selected LP formulations. Data are expressed as means ± SD, n = 3.

phosphatidylcholine and the surfactant equal to 85:15. As can be seen, EE% values of vesicles containing surfactants were greater with respect to those of LP ($p < 0.05$ with except for LP-T85 and LP-S80), reaching values greater than 80 %. This behaviour can be generally ascribed to surfactant ability to interact with AZT, improving its inclusion inside the vesicle bilayer, in agreement with previous findings (Duangjit et al., 2011). Similar results were also found where the employment of hydrophilic surfactants demonstrated high drug entrapment in vesicles (Fang et al., 2008). Tween 85 and Span 80 instead showed lower percentages compared to the other above-mentioned. Among Tweens and Spans, Tween 85 and Span 80 are the more lipophilic, and their presence in the vesicle bilayer can compete with the encapsulation of lipophilic molecules, like AZT (El Zaafarany et al., 2010). Moreover, the occurrence of double bonds within these surfactants has the potential to induce a bend in the alkyl chain of the vesicle bilayer. This, in turn, can result in a reduction in the domain capable of entrapment of the drug (Abdelbary and El-gendy, 2008; Khan et al., 2021). LP-T40, LP-T80, LP-S20 and LP-S60, showing the highest values of EE%, were selected for further studies.

3.3. *In vitro drug release*

In vitro drug release profiles can provide fundamental information about the formulation design, predicting, with due approximation, their behaviour as delivery systems. Given that the pH of the human vaginal environment is approximately 4.5, the drug release studies were conducted under these conditions (Giordani et al., 2019; Jøraholmen et al., 2020b).

Figs. 4A and 4B depict AZT release profiles from Tweens and Spans-containing formulations, respectively. Both LP and the control (CTRL) are shown as a comparison.

CTRL determined a rapid dissolution of the drug, reaching the maximum after 120 min. A more gradual drug release behaviour was observed for all the developed vesicles, due to the repartition process of the drug between the vesicle bilayer and the release medium (Abruzzo et al., 2024). Moreover, vesicle release profiles were characterised by a similar initial burst release within 30–60 min, probably due to the release of the non-encapsulated drug (Barbalho et al., 2024; Lei et al., 2013; Qushawy et al., 2018). The initial burst release can be considered advantageous because it permits to achievement of the therapeutic concentration in a short period (Hady et al., 2022; Ruckmani and Sankar, 2010). After this time, a more sustained release was observed, which may contribute to the maintenance of controlled drug concentrations within the vaginal cavity. Overall, among the Tween-containing vesicles, LP-T80 determined the release of the highest amount of drug. The double bond of T80 probably creates a bend in the vesicle bilayer, reducing the packing of the hydrophobic tails and consequently enhancing drug diffusion, in agreement with previous findings (Aboud et al., 2016; Ruckmani and Sankar, 2010). Regarding Span-containing vesicles, LP-S20 determined the release of the highest amount of drug, although no significant difference was observed with respect to LP ($p > 0.05$). This result can be attributed to the less lipophilic characteristic of Span 20 compared to the other Span surfactants, which allows for improving drug partitioning towards the release medium (Bayindir and Yuksel, 2010). Moreover, LP-S20 were distinguished for their smallest size among all the Span-containing vesicles. In the majority of cases, the presence of small vesicles is associated with a high surface area, thereby improving drug release (Aboud et al., 2016; Abruzzo et al., 2024). Considering the best release behaviours of LP-T80 and LP-S20, they were selected for the following tests.

3.4. *Transmission electron microscopy (TEM)*

Transmission electron microscopy allowed the evaluation of the shape, size, and membrane integrity of the vesicles, and the presence or absence of material within them. To evaluate their size, 20 vesicles of each sample were measured in 20 different areas, and the average of all the measurements was calculated. Fig. 5 reports TEM images of LP (A), LP-T80 (B) and LP-S20 (C). In Fig. 5A, the vesicles appear with well-preserved membranes and dimensions between 160 and 180 nm. The vesicles appear electron-dense, demonstrating the presence of lipophilic material within them. Fig. 5B shows vesicles with well-preserved membranes. They have dimensions between 130 and 140 nm and appear slightly less electron dense, probably due to the presence of the hydrophilic surfactant inside them. In Fig. 5C vesicles appear to have well-preserved membranes. They are electrondense and have dimensions between 200 and 210 nm. In general, this analysis confirmed the presence of roughly rounded vesicles, whose size measurements generally matched with PCS data.

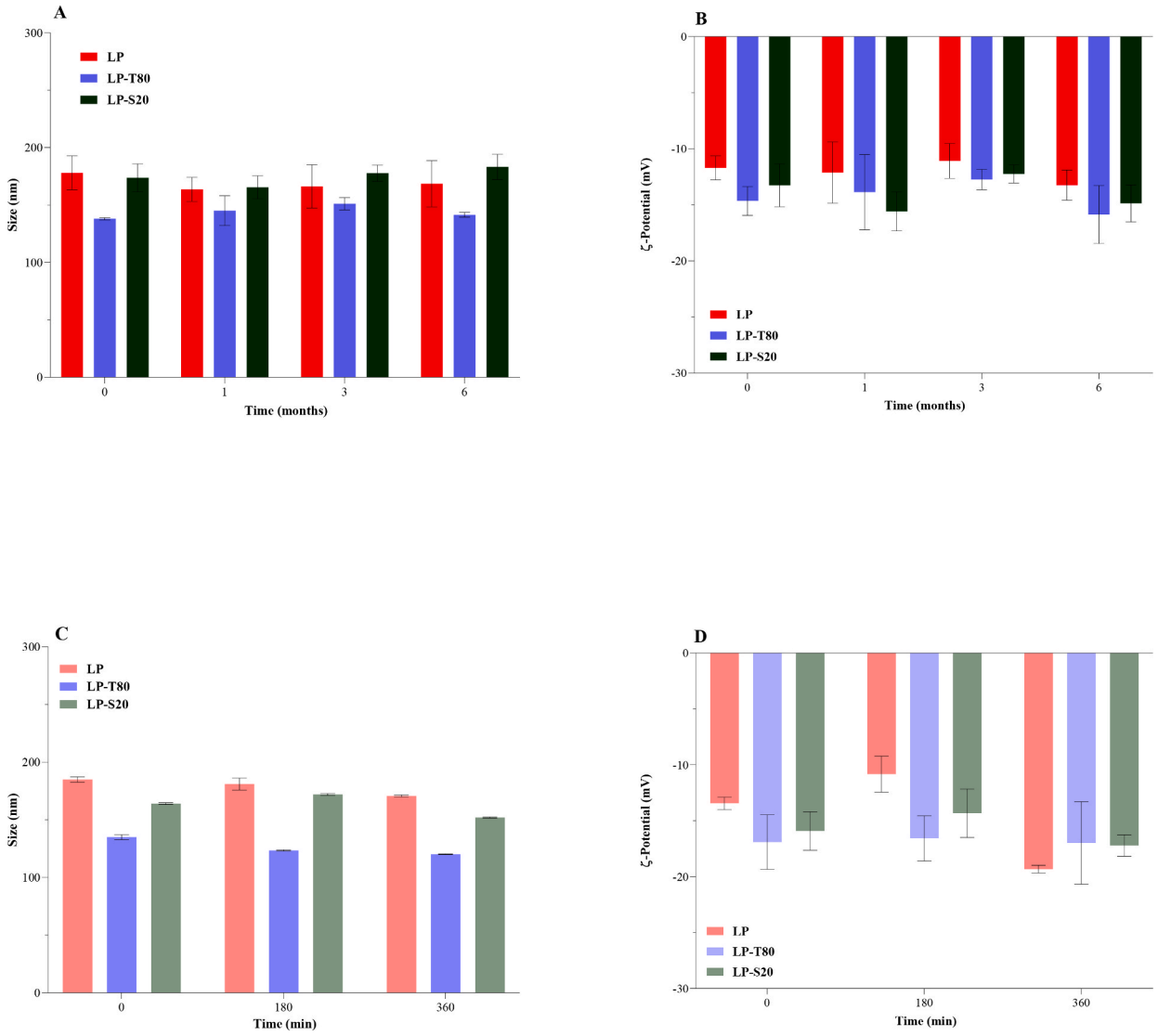

Fig. 7. Size (A) and ζ-potential (B) values after 1, 3, and 6 months compared to the fresh formulation. Data are expressed as means ± SD, n = 3. Size (C) and ζ-potential (D) values assessed in phosphate buffer at pH 4.5 (T = 37 °C) after 0, 180, and 360 min. Data are expressed as means ± SD, n = 3.

3.5. *Mucopenetrating properties*

In the field of treating vaginal infections, a promising formulation should closely contact the vaginal epithelium to achieve maximum efficacy of the drug. The macrolide antibiotic AZT inhibits bacterial protein synthesis by irreversibly binding to the 50S subunit of the ribosome. Due to its ability to accumulate within host cells and reach high intracellular concentrations, AZT is effective against Chlamydia species, which are obligate intracellular pathogens (Heidary et al., 2022). However, to fulfil its task, it must reach the cells of the vaginal epithelium, passing through the overlying mucus layer. Nevertheless, the presence of an outer luminal mucus layer, into which formulations can be trapped, generally obstructs the reaching of this goal. In this context, mucopenetrating vesicles can be considered an interesting option for vaginal drug delivery. Liposomes enriched with surfactant can diffuse through the mucus layer, depending on their size, surface charge and flexibility. In this study, the tube assay was utilised to evaluate vesicle penetration through mucus. This assay explores the vesicles' capacity to traverse a tube containing a mucin suspension. To detect vesicles during the diffusion, LP, LP-T80 and LP-S20 were prepared by including a fluorescent molecule, Lumogen red. A solution containing only Lumogen was also tested as a control. Size, PDI, and ζ-potential values of these vesicles did not differ from those containing AZT alone (data not shown, $p > 0.05$). As shown in Fig. 6, the control mainly remained close to the starting point of the tube (slices 2–8). Indeed, Lumogen can interact with the hydrophobic groups of mucin via hydrophobic and Van der Waals interactions, remaining trapped within the first part of the tube (Murgia et al., 2018; Sigurdsson et al., 2013; Witten et al., 2018). Conversely, all the vesicles diffused more deeply, reaching the middle/last sections of the mucin suspension. The latter result can be attributed to the vesicle's ability to diffuse within the mucus mesh pores (Boegh and Nielsen, 2015), in virtue of their reduced size and the slightly negative charges. As previously reported, nanosystems with mean diameters below the average mucus mesh pores, which is around 350 nm (Boegh and Nielsen, 2015), can diffuse deeper into the mucus layer. Moreover, in general, slightly negative or near neutral nanocarriers could diffuse and penetrate among the mesh more easily (Abruzzo et al., 2021; Rossi et al., 2019; Zheng et al., 2025) than the positive ones, which can interact with the negatively charged mucin. Among all the formulations, LP containing surfactant penetrated the mucus to a comparatively higher extent with respect to LP, reaching the last slice of the tube. This can probably be due to the surfactant ability to enhance the flexibility of the vesicle, facilitating their transport through mucus (Kanojiya et al., 2025).

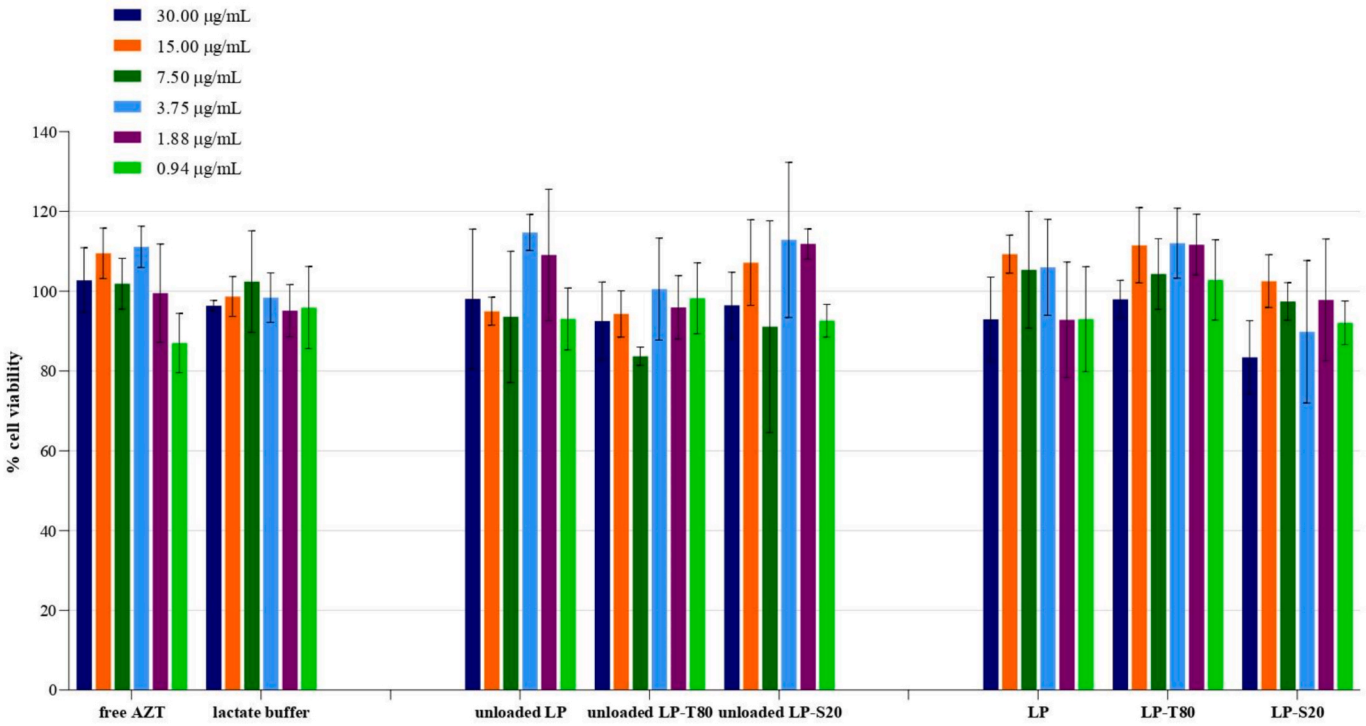

Fig. 8. Cytotoxicity of free AZT, unloaded liposomes, and AZT-loaded liposomes tested on HeLa cells (concentrations corresponding to 30–0.94 mg/mL of AZT), assessed by MTT assay after 48 h of treatment. Data are expressed as means ± SD percent of control (untreated cells, 100 %), n = 4.

Table 1
MIC (µg/mL) values of free AZT and AZT-loaded liposomes for *Chlamydia trachomatis* serovar D and serovar L. Anti-chlamydial activity tests were performed on HeLa cells.

Sample	MIC (µg/mL)	
	Serovar D	Serovar L
AZT	0.015	0.015
LP	0.0075–0.015	0.0075–0.015
LP-T80	0.0075–0.015	0.0075–0.015
LP-S20	0.0075–0.015	0.0075–0.015

3.6. Stability

Stability is a crucial parameter in the development of a drug delivery system. A stable dosage form preserves its physical structure and does not negatively affect the chemical stability of the active ingredient throughout its shelf life. In this study, the selected formulations were stored at 4–8 °C and monitored for 3 months. From a first visual inspection, no signs of aggregation were observed, and vesicle suspensions generally maintained their opalescent appearance. Figs. 7A and 7B report the size and ζ-potential values of the formulations measured during the storage period. By measuring their size, PDI (data not shown) and ζ-potential over time, no relevant changes were assessed. Surfactants with bulky hydrophilic heads, like Tweens, can impart strong steric repulsion, which reduces vesicle–vesicle interactions and aggregation, thereby improving colloidal stability. On the other hand, Span-containing vesicles maintained their properties because of their negative charges, which avoided vesicle aggregation. Along with the assessment of physical and chemical stability, we also evaluated the maintenance of the encapsulation efficiency for the selected formulations (LP, LP-T80 and LP-S20). After 6 months of storage, they still encapsulate the same amount of AZT as that present after their preparation (data not shown; $p < 0.05$), thus confirming their effective overall stability. Figs. 7C and 7D show the stability of the selected formulations in the phosphate buffer (37 °C) at pH 4.5, simulating the vaginal pH. As can be seen, no relevant variations in the measurements of size and ζ-potential were observed, thus confirming the formulation stability in the tested conditions.

3.7. Cytotoxicity assay

The cytotoxic profile of free AZT, lactate buffer, unloaded liposomes (unloaded LP, unloaded LP-T80, unloaded LP-S20), and AZT-loaded liposomes (LP, LP-T80, LP-S20) was assessed on HeLa cells by MTT assay. As can be seen from Fig. 8, HeLa cells' viability was not affected by free AZT, lactate buffer, as well as by unloaded and loaded liposomes at the tested concentrations; these results indicate that liposomes can be further tested for their anti-chlamydial activity in the same cellular model. These findings are consistent with a previous study showing that liposomal formulations exhibit biocompatibility in cervical cell models, maintaining high cell viability even at high concentrations (Vanić et al., 2019).

3.8. Evaluation of anti-chlamydial activity

In vitro experiments evaluating the activity of liposomal formulations against CT are essential, as they provide valuable insights into the interactions between liposomes and host cells. These studies are also useful for predicting potential *in vivo* efficacy.

Table 1 reports the MIC values (µg/mL) of free AZT and AZT-loaded liposomes. Identical MIC values were observed for both *Chlamydia* strains.

Our results indicate that all AZT-loaded liposomal formulations – both those composed solely of phosphatidylcholine (LP) and those incorporating surfactants from the Tween and Span series (LP-T80, LP-S20) – exhibited identical antimicrobial activity against both CT strains, with MIC values ranging from 0.0075 to 0.015 µg/mL. No statistically significant differences were observed among the different formulations or between the two strains. These findings are in line with previous studies reporting that various surface-charged elastic AZT

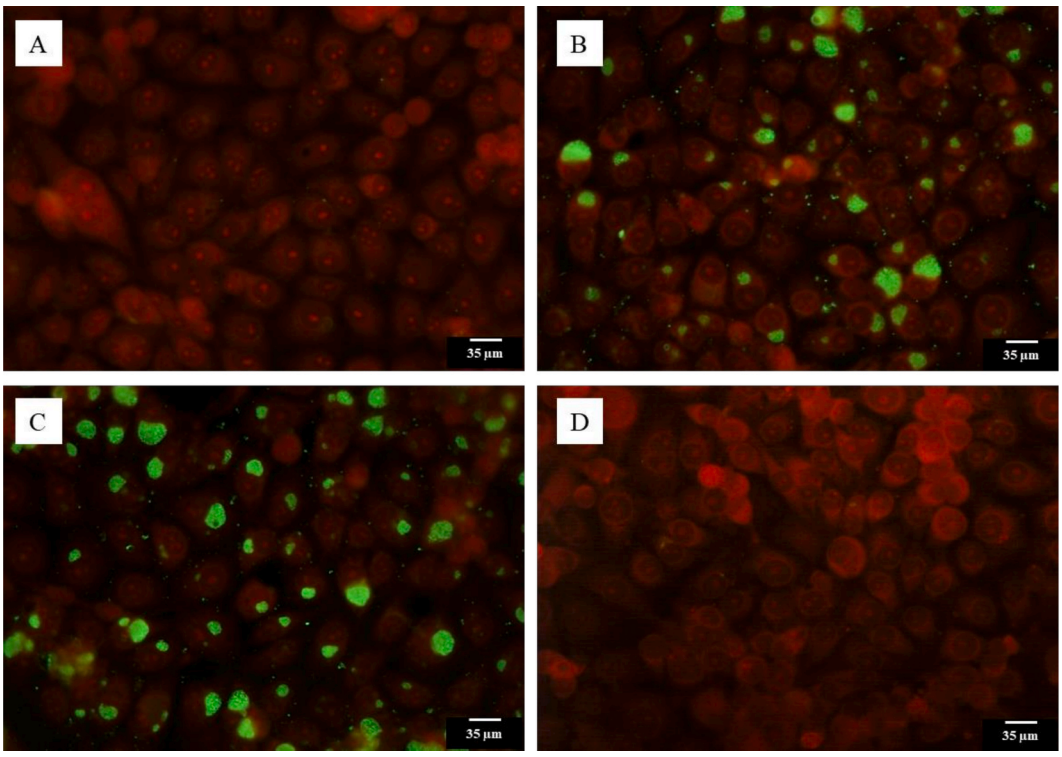

Fig. 9. Morphological analysis of HeLa cells. Representative micrographs of HeLa cells under different experimental conditions, observed under a fluorescence microscope (400 ×). (A) HeLa cells; (B) infected HeLa cells; (C) infected HeLa cells treated with unloaded LPT80; (D) infected HeLa cells treated with loaded LP-T80 at the MIC.

liposomes (neutral, cationic, and anionic) produced 2- to 8-fold reductions in MIC values compared to free AZT, with minimal variation among liposomal types (Bogdanov et al., 2021; Vanić et al., 2019).

Treatment with unloaded formulations and lactate buffer (under the same dilutions of loaded formulations) did not significantly affect chlamydial inclusion formation in HeLa cell, indicating a lack of antimicrobial activity.

Interestingly, AZT-loaded liposomes (MIC: 0.0075–0.015 µg/mL) exhibited slightly enhanced antimicrobial activity compared to free AZT (MIC: 0.015 µg/mL), despite identical MIC values across the liposomal formulations. This observation aligns with earlier reports demonstrating improved delivery and intracellular accumulation of AZT when encapsulated in liposomes, resulting in more effective bacterial inhibition (Lugli et al., 2025; Salem et al., 2005; Yıldırım and Düzgüneş, 2025).

To strengthen the evidence of biosafety, we complemented our data with morphological analyses of HeLa cells treated with the liposomal formulations. When observed under a fluorescence microscope, HeLa cells, treated with FITC-conjugated anti-chlamydial antibody and Evans blue, display a typical morphology, with a central nucleus of elongated shape and one or more nucleoli visible inside (Fig. 9A). Fig. 9B shows the characteristic cytoplasmic inclusions caused by *C. trachomatis* infection, which displace the nuclei toward the cell periphery; HeLa cells infected with *C. trachomatis* and treated with unloaded LP-T80 similarly exhibit the typical infection phenotype (Fig. 9C). Fig. 9D shows HeLa cells infected with *C. trachomatis* and treated with loaded LP-T80 at the measured MIC, which conversely presented a similar appearance to Fig. 9A.

4. Conclusion

Chlamydia infection, caused by the obligate pathogen *C. trachomatis*, has been associated with infertility, chronic pelvic pain and inflammation. These symptoms can result in reproductive tract damage if the infection is left untreated. In this study, we have developed a novel series of surfactant-enriched liposomes with the ultimate aim of obtaining mucopenetrating formulations that have the potential to ameliorate *Chlamydia* infections. The findings of this study demonstrate that the composition of liposomes exerts a significant influence on the chemical, physical, and functional characteristics of the resulting formulations. The presence of surfactants within the phospholipid bilayer has been shown to influence the size and surface charge of the vesicles, thus rendering them suitable for traversing mucus pores. Furthermore, the aforementioned excipients have been demonstrated to enhance drug release and improve mucopenetration ability in comparison to phosphatidylcholine-only liposomes. The evaluation of mucopenetrating properties, firstly proposed in this study, could pave the way to optimize the properties of drug delivery systems intended for vaginal application. Moreover, the compatibility of the formulation with HeLa cells, in conjunction with the enhancement of antimicrobial activity, lends support to the hypothesis that the obtained mucopenetrating liposomes can serve as an effective vaginal carrier for the local treatment of *C. trachomatis* infection.

CRediT authorship contribution statement

Sara Lugli: Writing – original draft, Methodology, Investigation, Formal analysis, Data curation, Conceptualization. **Angela Abruzzo:** Writing – original draft, Supervision, Resources, Formal analysis, Data curation, Conceptualization. **Carola Parolin:** Writing – original draft, Methodology, Investigation. **Beatrice Vitali:** Writing – review & editing. **Antonella Marangoni:** Writing – review & editing, Data curation, Conceptualization. **Marielle Ezekielle Djusse:** Writing – review & editing, Methodology, Investigation. **Michela Battistelli:** Writing – original draft, Methodology, Investigation, Data curation, Conceptualization. **Maria Laura Bolognesi:** Resources, Funding acquisition. **Teresa Cerchiara:** Writing – review & editing. **Barbara Luppi:** Writing – review & editing. **Federica Bigucci:** Writing – review & editing, Supervision, Resources, Data curation, Conceptualization.

Declaration of competing interest

The authors declare the following financial interests/personal relationships which may be considered as potential competing interests: Angela Abruzzo reports financial support was provided by EU – NextGenerationEU with funds made available by the National Recovery and Resilience Plan (NRRP) – Partenariati Estesi (PE13 – INF-ACT) – CUP J33C2200287000. Other authors declare that they have no known competing financial interests or personal relationships that could have appeared to influence the work reported in this paper.

Acknowledgements

The authors would like to thank Giulia Giacomozzi for her valuable contributions. This research was supported by EU within the NextGeneration EU-MUR PNRR Extended Partnership initiative on Emerging Infectious Diseases (Project no. PE00000007, INF-ACT) - CUP: J33C22002870005. Marielle Ezekielle Djusse was supported by the European Union-funded grant - NextGenerationEU from the National Recovery and Resilience Plan (NRRP) Mission 4, Component 1, Investment 3.4 (DM 118/2023) - Digital and Environmental Transitions - CUP: J33C23002390002.

Data availability

Data will be made available on request.

References

Abdelbary, G., El-gendy, N., 2008. Niosome-encapsulated gentamicin for ophthalmic controlled delivery. AAPS PharmSciTech 9, 740–747. https://doi.org/10.1208/s12249-008-9105-1.

Aboud, H.M., Ali, A.A., El-Menshawe, S.F., Elbary, A.A., 2016. Nanotransfersomes of carvedilol for intranasal delivery: formulation, characterization and *in vivo* evaluation. Drug Deliv. 23, 2471–2481. https://doi.org/10.3109/10717544.2015.1013587.

Abruzzo, A., Giordani, B., Miti, A., Vitali, B., Zuccheri, G., Cerchiara, T., Luppi, B., Bigucci, F., 2021. Mucoadhesive and mucopenetrating chitosan nanoparticles for glycopeptide antibiotic administration. Int. J. Pharm. 606, 120874. https://doi.org/10.1016/j.ijpharm.2021.120874.

Abruzzo, A., Pucci, R., Abruzzo, P.M., Canaider, S., Parolin, C., Vitali, B., Valle, F., Brucale, M., Cerchiara, T., Luppi, B., Bigucci, F., 2024. Azithromycin-loaded liposomes and niosomes for the treatment of skin infections: Influence of excipients and preparative methods on the functional properties. Eur. J. Pharm. Biopharm. 197, 114233. https://doi.org/10.1016/j.ejpb.2024.114233.

Albash, R., Elmahboub, Y., Baraka, K., Abdellatif, M.M., Alaa-Eldin, A.A., 2020. Ultradeformable liposomes containing terpenes (terpesomes) loaded fenticonazole nitrate for treatment of vaginal candidiasis: Box-Behnken design optimization, comparative *ex vivo* and *in vivo* studies. Drug Deliv. 27, 1514–1523. https://doi.org/10.1080/10717544.2020.1837295.

Antimisiaris, S.G., Marazioti, A., Kannavou, M., Natsaridis, E., Gkartziou, F., Kogkos, G., Mourtas, S., 2021. Overcoming barriers by local drug delivery with liposomes. Adv. Drug Deliv. Rev. 174, 53–86. https://doi.org/10.1016/j.addr.2021.01.019.

Barbalho, G.N., Brugger, S., Raab, C., Lechner, J.-S., Gratieri, T., Keck, C.M., Rupenthal, I.D., Agarwal, P., 2024. Development of transferosomes for topical ocular drug delivery of curcumin. Eur. J. Pharm. Biopharm. 205, 114535. https://doi.org/10.1016/j.ejpb.2024.114535.

Bayindir, Z.S., Yuksel, N., 2010. Characterization of niosomes prepared with various nonionic surfactants for paclitaxel oral delivery. J. Pharm. Sci. 99, 2049–2060. https://doi.org/10.1002/jps.21944.

Bnyan, R., Khan, I., Ehtezazi, T., Saleem, I., Gordon, S., O'Neill, F., Roberts, M., 2019. Formulation and optimisation of novel transfersomes for sustained release of local anaesthetic. J. Pharm. Pharmacol. 71, 1508–1519. https://doi.org/10.1111/jphp.13149.

Bnyan, R., Khan, I., Ehtezazi, T., Saleem, I., Gordon, S., O'Neill, F., Roberts, M., 2018. Surfactant effects on lipid-based vesicles properties. J. Pharm. Sci. 107, 1237–1246. https://doi.org/10.1016/j.xphs.2018.01.005.

Boegh, M., Nielsen, H.M., 2015. Mucus as a barrier to drug delivery – understanding and mimicking the barrier properties. Basic Clin. Pharmacol. Toxicol. 116, 179–186. https://doi.org/10.1111/bcpt.12342.

Bogdanov, Janovák, L., Vraneš, J., Meštrović, T., Ljubin-Sternak, S., Cseh, Z., Endrész, V., Burián, K., Vanić, Ž., Virok, D.P., 2021. Liposomal encapsulation increases the efficacy of azithromycin against chlamydia trachomatis. Pharmaceutics 14, 36. https://doi.org/10.3390/pharmaceutics14010036.

Briuglia, M.-L., Rotella, C., McFarlane, A., Lamprou, D.A., 2015. Influence of cholesterol on liposome stability and on in vitro drug release. Drug Deliv. Transl. Res. 5, 231–242. https://doi.org/10.1007/s13346-015-0220-8.

Crisóstomo, L.C.C.F., Carvalho, G.S.G., Leal, L.K.A.M., De Araújo, T.G., Nogueira, K.A.B., Da Silva, D.A., De Oliveira Silva Ribeiro, F., Petrilli, R., Eloy, J.O., 2022. Sorbitan monolaurate–containing liposomes enhance skin cancer cell cytotoxicity and in association with microneedling increase the skin penetration of 5-fluorouracil. AAPS PharmSciTech 23, 212. Doi: 10.1208/s12249-022-02356-z.

De Gregorio, P.R., Parolin, C., Abruzzo, A., Luppi, B., Protti, M., Mercolini, L., Silva, J.A., Giordani, B., Marangoni, A., Nader-Macías, M.E.F., Vitali, B., 2020. Biosurfactant from vaginal Lactobacillus crispatus BC1 as a promising agent to interfere with Candida adhesion. Microb. Cell Factories 19, 133. https://doi.org/10.1186/s12934-020-01390-5.

Duangjit, S., Opanasopit, P., Rojanarata, T., Ngawhirunpat, T., 2011. Characterization and *in vitro* skin permeation of meloxicam-loaded liposomes versus transfersomes. J. Drug Deliv. 2011, 1–9. https://doi.org/10.1155/2011/418316.

Duangjit, S., Opanasopit, P., Rojanarata, T., Obata, Y., Takayama, K., Ngawhirunpat, T., Pamornpathomkul, B., 2014. Role of the charge, carbon chain length, and content of surfactant on the skin penetration of meloxicam-loaded liposomes. Int. J. Nanomed. 2005. https://doi.org/10.2147/IJN.S60674.

El Zaafarany, G.M., Awad, G.A.S., Holayel, S.M., Mortada, N.D., 2010. Role of edge activators and surface charge in developing ultradeformable vesicles with enhanced skin delivery. Int. J. Pharm. 397, 164–172. https://doi.org/10.1016/j.ijpharm.2010.06.034.

Fang, Y.-P., Tsai, Y.-H., Wu, P.-C., Huang, Y.-B., 2008. Comparison of 5-aminolevulinic acid-encapsulated liposome versus ethosome for skin delivery for photodynamic therapy. Int. J. Pharm. 356, 144–152. https://doi.org/10.1016/j.ijpharm.2008.01.020.

Filardo, S., Di Pietro, M., Sessa, R., 2022. Better in vitro tools for exploring chlamydia trachomatis pathogenesis. Life 12, 1065. https://doi.org/10.3390/life12071065.

Foschi, C., Bortolotti, M., Marziali, G., Polito, L., Marangoni, A., Bolognesi, A., 2019. Survival and death of intestinal cells infected by Chlamydia trachomatis. PLoS One 14, e0215956. https://doi.org/10.1371/journal.pone.0215956.

Foschi, C., Laghi, L., D'Antuono, A., Gaspari, V., Zhu, C., Dellarosa, N., Salvo, M., Marangoni, A., 2018. Urine metabolome in women with Chlamydia trachomatis infection. PLoS One 13, e0194827. https://doi.org/10.1371/journal.pone.0194827.

Giordani, B., Basnet, P., Mishchenko, E., Luppi, B., Škalko-Basnet, N., 2019. Utilizing liposomal quercetin and gallic acid in localized treatment of vaginal candida infections. Pharmaceutics 12, 9. https://doi.org/10.3390/pharmaceutics12010009.

Gupta, A., 2012. Transfersomes: a novel vesicular carrier for enhanced transdermal delivery of sertraline: development, characterization, and performance evaluation. Sci. Pharm. 80, 1061–1080. https://doi.org/10.3797/scipharm.1208-02.

Hady, M.A., Darwish, A.B., Abdel-Aziz, M.S., Sayed, O.M., 2022. Design of transfersomal nanocarriers of nystatin for combating vulvovaginal candidiasis; a different prospective. Colloids Surf. B Biointerfaces 211, 112304. https://doi.org/10.1016/j.colsurfb.2021.112304.

Heidary, M., Ebrahimi Samangani, A., Kargari, A., Kiani Nejad, A., Yashmi, I., Motahar, M., Taki, E., Khoshnood, S., 2022. Mechanism of action, resistance, synergism, and clinical implications of azithromycin. J. Clin. Lab. Anal. 36, e24427. https://doi.org/10.1002/jcla.24427.

Hofland, H.E.J., Bouwstra, J.A., Gooris, G.S., Spies, F., Talsma, H., Junginger, H.E., 1993. Nonionic surfactant vesicles: a study of vesicle formation, characterization, and stability. J. Colloid Interface Sci. 161, 366–376. https://doi.org/10.1006/jcis.1993.1479.

Jøraholmen, M.W., Bhargava, A., Julin, K., Johannessen, M., Škalko-Basnet, N., 2020a. The antimicrobial properties of chitosan can be tailored by formulation. Mar. Drugs 18, 96. https://doi.org/10.3390/md18020096.

Jøraholmen, M.W., Johannessen, M., Gravningen, K., Puolakkainen, M., Acharya, G., Basnet, P., Škalko-Basnet, N., 2020b. Liposomes-in-hydrogel delivery system enhances the potential of resveratrol in combating vaginal chlamydia infection. Pharmaceutics 12, 1203. https://doi.org/10.3390/pharmaceutics12121203.

Kanojiya, P.S., Wadetwar, R.N., Atole, P.G., Thakrani, K.C., Gawande, N.P., 2025. Sustained delivery of statistically optimized transfersomal gel of miconazole nitrate for vaginal candidiasis. J. Dispers. Sci. Technol. 46, 333–350. https://doi.org/10.1080/01932691.2023.2289621.

Khan, I., Needham, R., Yousaf, S., Houacine, C., Islam, Y., Bnyan, R., Sadozai, S.K., Elrayess, M.A., Elhissi, A., 2021. Impact of phospholipids, surfactants and cholesterol selection on the performance of transfersomes vesicles using medical nebulizers for pulmonary drug delivery. J. Drug Deliv. Sci. Technol. 66, 102822. https://doi.org/10.1016/j.jddst.2021.102822.

Kim, J., Ślęczkowska, M., Nobre, B., Wieringa, P., 2025. Study models for chlamydia trachomatis infection of the female reproductive tract. Microorganisms 13, 553. https://doi.org/10.3390/microorganisms13030553.

Kopermsub, P., Mayen, V., Warin, C., 2011. Potential use of niosomes for encapsulation of nisin and EDTA and their antibacterial activity enhancement. Food Res. Int. 44, 605–612. https://doi.org/10.1016/j.foodres.2010.12.011.

Lei, W., Yu, C., Lin, H., Zhou, X., 2013. Development of tacrolimus-loaded transfersomes for deeper skin penetration enhancement and therapeutic effect improvement in vivo. Asian J. Pharm. Sci. 8, 336–345. https://doi.org/10.1016/j.ajps.2013.09.005.

Li, D., Vaglenov, A., Kim, T., Wang, C., Gao, D., Kaltenboeck, B., 2005. High-yield culture and purification of Chlamydiaceae bacteria. J. Microbiol. Methods 61, 17–24. https://doi.org/10.1016/j.mimet.2004.10.020.

Liu, D., Hu, H., Lin, Z., Chen, D., Zhu, Y., Hou, S., Shi, X., 2013. Quercetin deformable liposome: preparation and efficacy against ultraviolet B induced skin damages in vitro and in vivo. J. Photochem. Photobiol. B 127, 8–17. https://doi.org/10.1016/j.jphotobiol.2013.07.014.

Liu, L., Tian, C., Dong, B., Xia, M., Cai, Y., Hu, R., Chu, X., 2021. Models to evaluate the barrier properties of mucus during drug diffusion. Int. J. Pharm. 599, 120415. https://doi.org/10.1016/j.ijpharm.2021.120415.

Lopez-Vidal, L., Juskaite, K., Ramöller, I.K., Real, D.A., McKenna, P.E., Priotti, J., Donnelly, R.F., Paredes, A.J., 2025. Advanced drug delivery systems for the management of local conditions. Ther. Deliv. 16, 285–303. https://doi.org/10.1080/20415990.2024.2437978.

Lugli, S., Abruzzo, A., Parolin, C., Vitali, B., Bolognesi, M.L., Brucale, M., Valle, F., Cerchiara, T., Luppi, B., Bigucci, F., 2025. Mucoadhesive polymer-coated liposomes as a promising approach to counteract bacteria responsible for aerobic vaginitis. Int. J. Pharm. 677, 125667. https://doi.org/10.1016/j.ijpharm.2025.125667.

Martín-Bartolomé, L., Ruiz-Caro, R., Veiga, M.D., Notario-Pérez, F., 2024. Evaluation of polymer combinations in vaginal mucoadhesive tablets for the extended release of acyclovir. Eur. J. Pharm. Sci. 203, 106919. https://doi.org/10.1016/j.ejps.2024.106919.

Murgia, X., Loretz, B., Hartwig, O., Hittinger, M., Lehr, C.-M., 2018. The role of mucus on drug transport and its potential to affect therapeutic outcomes. Adv. Drug Deliv. Rev. 124, 82–97. https://doi.org/10.1016/j.addr.2017.10.009.

Nardini, P., Ñahui Palomino, R.A., Parolin, C., Laghi, L., Foschi, C., Cevenini, R., Vitali, B., Marangoni, A., 2016. Lactobacillus crispatus inhibits the infectivity of Chlamydia trachomatis elementary bodies, in vitro study. Sci. Rep. 6, 29024. https://doi.org/10.1038/srep29024.

Onyesom, I., Lamprou, D.A., Sygellou, L., Owusu-Ware, S.K., Antonijevic, M., Chowdhry, B.Z., Douroumis, D., 2013. Sirolimus encapsulated liposomes for cancer therapy: physicochemical and mechanical characterization of sirolimus distribution within liposome bilayers. Mol. Pharm. 10, 4281–4293. https://doi.org/10.1021/mp400362v.

Pacheco-Quito, E.-M., Ruiz-Caro, R., Rubio, J., Tamayo, A., Veiga, M.-D., 2020. Carrageenan-based acyclovir mucoadhesive vaginal tablets for prevention of genital herpes. Mar. Drugs 18, 249. https://doi.org/10.3390/md18050249.

Pandey, Pandey, T., Khan, S., Wamankar, S., 2024. Enhancement of Low Solubility and Low Permeability Drug Azithromycin Using Crystallization Techniques 917–921.

Qushawy, M., Nasr, A., Abd-Alhaseeb, M., Swidan, S., 2018. Design, optimization and characterization of a transfersomal gel using miconazole nitrate for the treatment of candida skin infections. Pharmaceutics 10, 26. https://doi.org/10.3390/pharmaceutics10010026.

Refai, H., Hassan, D., Abdelmonem, R., 2017. Development and characterization of polymer-coated liposomes for vaginal delivery of sildenafil citrate. Drug Deliv. 24, 278–288. https://doi.org/10.1080/10717544.2016.1247925.

Rossi, S., Vigani, B., Sandri, G., Bonferoni, M.C., Caramella, C.M., Ferrari, F., 2019. Recent advances in the mucus-interacting approach for vaginal drug delivery: from mucoadhesive to mucus-penetrating nanoparticles. Expert Opin. Drug Deliv. 16, 777–781. https://doi.org/10.1080/17425247.2019.1645117.

Ruckmani, K., Sankar, V., 2010. Formulation and optimization of zidovudine niosomes. AAPS PharmSciTech 11, 1119–1127. https://doi.org/10.1208/s12249-010-9480-2.

Salem, I.I., Flasher, D.L., Düzgüneş, N., 2005. Liposome-Encapsulated Antibiotics, in: Methods in Enzymology. Elsevier, pp. 261–291. Doi: 10.1016/S0076-6879(05)91015-X.

Shapiro, R.L., DeLong, K., Zulfiqar, F., Carter, D., Better, M., Ensign, L.M., 2022. In vitro and ex vivo models for evaluating vaginal drug delivery systems. Adv. Drug Deliv. Rev. 191, 114543. https://doi.org/10.1016/j.addr.2022.114543.

Sigurdsson, H.H., Kirch, J., Lehr, C.-M., 2013. Mucus as a barrier to lipophilic drugs. Int. J. Pharm. 453, 56–64. https://doi.org/10.1016/j.ijpharm.2013.05.040.

Singh, S., Verma, D., Mirza, Mohd.A., Das, A.K., dudeja, M., Anwer, Md.K., Sultana, Y., Talegaonkar, S., Iqbal, Z., 2017. Development and optimization of ketoconazole loaded nano-transfersomal gel for vaginal delivery using Box-Behnken design: In vitro , ex vivo characterization and antimicrobial evaluation. J. Drug Deliv. Sci. Technol. 39, 95–103. Doi: 10.1016/j.jddst.2017.03.007.

Squittieri, R., Baldino, L., Reverchon, E., 2023. Production of antioxidant transfersomes by a supercritical CO2 assisted process for transdermal delivery applications. Nanomaterials 13, 1812. https://doi.org/10.3390/nano13121812.

Tasi, L.-M., Liu, D.-Z., Chen, W.-Y., 2003. Microcalorimetric investigation of the interaction of polysorbate surfactants with unilamellar phosphatidylcholines liposomes. Colloids Surf. Physicochem. Eng. Asp. 213, 7–14. https://doi.org/10.1016/S0927-7757(02)00287-X.

Tidbury, F., Brülhart, G., Müller, G., Pavicic, E., Weidlinger, S., Eichner, G., Von Wolff, M., Stute, P., 2025. Effectiveness and tolerability of lactic acid vaginal gel compared to oral metronidazole in the treatment of acute symptomatic bacterial vaginosis: a multicenter, randomized-controlled, head-to-head pilot study. BMC Womens Health 25. https://doi.org/10.1186/s12905-024-03513-1.

Ullmann, K., Leneweit, G., Nirschl, H., 2021. How to achieve high encapsulation efficiencies for macromolecular and sensitive APIs in liposomes. Pharmaceutics 13, 691. https://doi.org/10.3390/pharmaceutics13050691.

Vanić, Ž., Hafner, A., Bego, M., Škalko-Basnet, N., 2013. Characterization of various deformable liposomes with metronidazole. Drug Dev. Ind. Pharm. 39, 481–488. https://doi.org/10.3109/03639045.2012.670247.

Vanić, Ž., Jøraholmen, M.W., Škalko-Basnet, N., 2025. Challenges and considerations in liposomal hydrogels for the treatment of infection. Expert Opin. Drug Deliv. 22, 255–276. https://doi.org/10.1080/17425247.2025.2451620.

Vanić, Ž., Rukavina, Z., Manner, S., Fallarero, A., Uzelac, L., Kralj, M., Amidžić Klarić, D., Bogdanov, A., Raffai, T., Virok, D.P., Filipović-Grčić, J., Škalko-Basnet, N., 2019. Azithromycin-liposomes as a novel approach for localized therapy of cervicovaginal bacterial infections. Int. J. Nanomed. 14, 5957–5976. https://doi.org/10.2147/IJN.S211691.

Walker, F.C., Derré, I., 2024. Contributions of diverse models of the female reproductive tract to the study of Chlamydia trachomatis-host interactions. Curr. Opin. Microbiol. 77, 102416. https://doi.org/10.1016/j.mib.2023.102416.

Wang, L., Fan, L., Yi, K., Jiang, Y., Filppula, A.M., Zhang, H., 2023. Advances in the delivery systems for oral antibiotics. Biomed. Technol. 2, 49–57. https://doi.org/10.1016/j.bmt.2022.11.010.

WHO, 2025. Sexually transmitted infections (STIs).

Witten, J., Samad, T., Ribbeck, K., 2018. Selective permeability of mucus barriers. Curr. Opin. Biotechnol. 52, 124–133. https://doi.org/10.1016/j.copbio.2018.03.010.

Wyrick, P.B., 2000. Intracellular survival by Chlamydia. Microreview. Cell. Microbiol. 2, 275–282. https://doi.org/10.1046/j.1462-5822.2000.00059.x.

Yasin, B., Pang, M., Wagar, E.A., Lehrer, R.I., 2002. Examination of chlamydia trachomatis infection in environments mimicking normal and abnormal vaginal pH. Sex. Transm. Dis. 29, 514–519. https://doi.org/10.1097/00007435-200209000-00004.

Yıldırım, M., Düzgüneş, N., 2025. Liposome-encapsulated antibiotics for the therapy of mycobacterial infections. Antibiotics 14, 728. https://doi.org/10.3390/antibiotics14070728.

Zheng, B., Liu, D., Qin, X., Zhang, D., Zhang, P., 2025. Mucoadhesive-to-mucopenetrating nanoparticles for mucosal drug delivery: a mini review. Int. J. Nanomed. 20, 2241–2252. https://doi.org/10.2147/IJN.S505427.